Tryptophan Substitutions Surrounding the Nucleotide in Catalytic Sites of F_1-ATPase†

Joachim Weber, Susan Wilke-Mounts, Sean T. Hammond, and Alan E. Senior*

Department of Biochemistry and Biophysics, Box 712, University of Rochester Medical Center, Rochester, New York 14642

Received May 11, 1998; Revised Manuscript Received June 18, 1998

ABSTRACT: Novel tryptophan substitutions, surrounding the nucleotide bound in catalytic sites, were introduced into *Escherichia coli* F_1-ATPase. The mutant enzymes were purified and studied by fluorescence spectroscopy. One cluster of Trp substitutions, consisting of β-Trp-404, β-Trp-410, β-Asp-158 (lining the adenine-binding pocket), and β-Trp-153 (close to the α/β-phosphates), showed the same fluorescence responses to MgADP, MgAMPPNP, and MgATP and the same nucleotide binding pattern with MgADP and MgAMPPNP, with one site of higher and two sites of lower affinity. Therefore, in absence of catalytic turnover (and of γ-subunit rotation), sites 2 and 3 appeared similar in affinity, and the region of the catalytic site sensed by these Trp substitutions did not change conformation with different nucleotides. In contrast, α-Trp-291 and β-Trp-297, both close to the γ-phosphate, showed very different fluorescence responses to MgADP versus MgAMPPNP, and in these cases the response was due exclusively or predominantly to nucleotide binding at the first, high-affinity catalytic site, thus allowing specific detection of this site. Titration with MgATP showed that the high-affinity site was present under conditions of steady-state, V_{max} MgATP hydrolysis.

ATP synthase (F_1F_o-ATPase) catalyzes ATP synthesis in the last step of oxidative phosphorylation in membranes of bacteria, mitochondria, and chloroplasts. In bacteria, when metabolic conditions dictate, the enzyme also hydrolyzes ATP to generate a transmembrane proton gradient (*1*, *2*). The enzyme consists of two sectors, the membrane-extrinsic F_1 and membrane-embedded F_o. There are three catalytic sites, located on F_1, each formed primarily from residues of β-subunit but situated at an interface between β and α (*3*). F_1 can be released from F_o and purified in soluble form with retention of ATPase activity, providing a widely used source material for experimental studies. A recent paper from our laboratory compared intact F_1F_o with isolated F_1 and established that the two preparations show essentially the same catalytic site nucleotide-binding characteristics (*4*).

In both F_1F_o and F_1, the three catalytic sites show strong binding cooperativity (asymmetry) toward substrate MgATP, with widely different K_d values at sites 1, 2, and 3, of <50 nM, 1 μM, and 30 μM, respectively. At cellular concentration of MgATP (~3 mM in *Escherichia coli*), all three catalytic sites are filled by nucleotide. Physiological rates of catalysis are only achieved when all three sites are occupied (*4*, *5*). Understanding the detailed properties of the three catalytic sites and how they work together in sequential fashion (*6*, *7*) to synthesize or hydrolyze ATP is central to establishing the catalytic mechanism. Current models of the enzyme mechanism envisage that, under steady-state turnover conditions, each of the three catalytic sites exists in a different conformation at any given moment in time, and that just one, the site of highest affinity, is catalytically active (*2*, *3*, *8*−*10*).

X-ray structural analysis (*3*, *11*−*13*) has provided a firm foundation for studies of specific catalytic site residues by mutagenesis and an approach that our laboratory has used is site-directed tryptophan fluorescence, in which Trp residues are substituted at specific positions to provide fluorescent probes of catalytic site occupancy. In one example of this technique, substitution of residue β-Tyr-331 → Trp[1] provided a sensitive fluorescent probe of true equilibrium binding of nucleotide by virtue of direct van der Waals contact between residue β-331 and the adenine ring of the bound nucleotide (*3*, *14*). Binding of a wide variety of nucleotide substrates and analogues was characterized (*5*, *14*−*16*).[2] Combination of the βY331W mutation with other catalytic site mutations provided a particularly incisive approach, allowing functional roles of individual side chains surrounding the γ-phosphate and the Mg^{2+} in MgATP to be determined (*14*, *15*, *21*). In a second example, substitution of residue β-Phe-148 → Trp (situated adjacent to the "P-loop") provided a fluorescent probe which could distinguish between MgATP and MgADP bound in catalytic sites, by virtue of opposite fluorescence responses to the two nucleotides (*22*). This allowed determination that, during steady-state ATP hydrolysis, in time average, one of the three catalytic sites contains MgATP while the other two sites contain MgADP.

It seemed likely that introduction of novel Trp residues at positions surrounding the catalytic site nucleotide would yield

† Supported by NIH grant GM25349 to A.E.S.

* Author to whom correspondence should be addressed.

[1] Residue numbers refer to *E. coli* enzyme.

[2] A parallel approach was developed for studies of nucleotide-binding in the three F_1 noncatalytic sites, utilizing the substitution α-Arg-365 → Trp (refs *17*−*20*). The hydrophobic, aliphatic side chain of α-Arg-365 makes contact with the adenine ring of bound nucleotide in noncatalytic sites (*3*).

S0006-2960(98)01089-7 CCC: $15.00
Published on Web 08/14/1998

Table 1: Oligonucleotides for Site-Directed Mutagenesis[a]

βY297W	TACAGGCAGTA*TGG*GTACCTGC	Inserts *KpnI* site
βF404W	CTGTCCCAGCC*AT**GG*TTCGTGGC	Inserts *NcoI* site
βF410W	TGGCAGAAGTA*TGG*AC*T*GGTTCTCC	Removes *AgeI* site
αF291W	GGGCGACGTTT*GG*TACCTCCACT	Inserts *KpnI* site
αF354W	GATGGTCAGAT*TT**GG*CTGGAAAC	Removes *BglII* site

[a] Italicized bases indicate change from wild-type sequence.

further information. Therefore, we carried out a study in which Trp residues were substituted in *E. coli* F_1 at positions close to the adenine ring, ribose, α/β-phosphates, and γ-phosphate of bound nucleotide, and the fluorescence responses of the purified mutant enzymes were characterized.

EXPERIMENTAL PROCEDURES

E. coli Mutant Strains. Site-directed mutagenesis was performed by the method of Vandeyar et al. (*23*) using the T7-GEN mutagenesis kit (USB). For β-subunit mutations, the template was M13mp18 containing the *Hind*III−*Kpn*I fragment from plasmid p0W1 (*24*), and each new mutation was transferred into plasmid p0W1 on an *Nhe*I−*Kpn*I or *Nhe*I−*Eag*I fragment. For α-subunit mutations the template was M13mp18 containing the *Sph*I−*Sal*I fragment from plasmid pDP34 (*21*), and each new mutation was transferred into plasmid p0W1 on a *Xho*I−*Csp*45I fragment. The final mutant plasmids were transformed into strain AN888 for growth tests and purification of F_1. In all cases, correct mutagenesis was confirmed by DNA sequencing, also several independent isolates were checked by growth tests. Oligonucleotides were as in Table 1; screening for the mutation was facilitated by insertion or removal of a restriction site. Generation of the βV153W and βN158W mutations was described in ref *22*.

Enzyme Purification and Characterization. Mutant and wild-type F_1 was prepared according to Weber et al. (*25*). Wild-type was from strain SWM1 (*26*). Purity and subunit composition of F_1 preparations was checked by SDS−gel electrophoresis (*27*). Protein concentrations of F_1 solutions were determined using the Bio-Rad protein assay (*28*).

Assays of Enzyme Function. Growth yield analyses in limiting (3 mM) glucose and tests of growth on solid succinate medium were performed as described (*29*). Standard ATPase activities were assayed in 50 mM Tris/H_2SO_4, 10 mM ATP, and 4 mM $MgSO_4$, pH 8.5, at 30 °C. Dependence of enzyme activity on substrate concentration was measured in buffer containing 50 mM Tris/H_2SO_4, pH 8.0, with varying concentrations of ATP (0.02−10 mM) and $MgSO_4$ (0.008−4 mM) in constant ratio of 2.5:1. Released P_i was determined by colorimetric assays (*30*, *31*).

Tryptophan Fluorescence Measurements. The experiments were carried out at 23 °C in spectrofluorometers type SPEX Fluorolog 2 or AMINCO Bowman 2. The excitation wavelength was 295 nm. Before use, the enzyme was preequilibrated in 50 mM Tris/H_2SO_4, pH 8.0, by consecutive passage through two 1 mL Sephadex G-50 centrifuge columns. This procedure was used previously to obtain enzyme with empty catalytic sites (*15*). In the experiments with MgADP and MgAMPPNP, the same buffer was used, with 2.5 mM $MgSO_4$ added. In cases where the nucleotide concentration exceeded 1.5 mM, an excess of 1 mM $MgSO_4$ over nucleotide was used. For MgATP, ATP and $MgSO_4$ were added at a constant ratio of 2.5:1. Concentrations of MgATP and MgAMPPNP were calculated using a dissociation constant of 20 μM; for MgADP, the dissociation constant used was 78 μM (*32*). F_1 concentration in the cuvette was 100−200 nM. Background signals (buffer) were subtracted; inner-filter and volume effects were corrected for by performing parallel titrations with wild-type F_1. With MgATP as the ligand, maximally two data points were acquired in a single experiment, to avoid interference by hydrolysis product MgADP. Binding parameters were determined by fitting theoretical curves to the measured data points. Several binding models were tested for each enzyme. In all cases, a model with either a single type of site or one with two types of site was sufficient to describe the binding behavior, no significant improvement being seen with a model encompassing three types of site.

RESULTS

Design of Tryptophan Substitutions. The aim of this work was to introduce Trp residues at positions surrounding nucleotide bound in the catalytic sites of *E. coli* F_1-ATPase, to characterize the effects of the novel Trp residues on cell growth and enzyme activity, and to examine the fluorescence signals of purified F_1 from the mutants, looking particularly for enzymes with novel properties. We identified initially aromatic residues located within 12 Å of MgAMPPNP bound in the catalytic site in the X-ray structure (*3*). β-Phe-404 and β-Phe-410, together with β-Tyr-331, line the adenine-binding pocket and are close to the adenine ring, with β-Phe-410 also coming close to the ribose; α-Phe-354, located on α-subunit, lies opposite to the ribose moiety of catalytic-site-bound nucleotide; and β-Tyr-297 and α-Phe-291 are located close to the γ-phosphate. In addition, we subjected purified F_1 from the mutants βV153W and βN158W to more detailed fluorescence characterization. These two mutations had been generated earlier (*22*) but had been studied only briefly.[3] Both lie in close proximity to the bound nucleotide, the former to the α- and β-phosphates and the latter to the adenine ring.

[3] The following mutants were also generated, but were not investigated in detail for the reasons stated: βG150W was fully Unc^- in succinate plate or growth yield tests, in Trp-free (p0W1) or wild-type background; βF312W and βY190W were Unc^+ in growth tests but failed to yield any purified F_1 for fluorescence studies, apparently due to instability of soluble enzyme.

Table 2: Properties of the Novel Tryptophan Mutants

mutation[a]	growth on succinate	growth yield in 3 mM glucose (%)	F_1-ATPase activity		
			V_{max} (units/mg)	K_M (μM)	k_{cat}/K_M (M^{-1} s^{-1})
wild-type[b]	++++	100	28	90	2.0×10^6 (100)[c]
p0W1/AN888	++++	100	46	180	1.6×10^6 (82)
Unc$^-$ [b]	−	55			
βY297W	++++	92	4.8	80	3.8×10^5 (19)
βF404W	++	79	14	265	3.4×10^5 (17)
βF410W	++++	98	20	160	8.0×10^5 (40)
αF291W	++++	97	36	70	3.3×10^6 (165)
αF354W	++++	101	31	280	7.0×10^5 (36)
βV153W[d]	++	74	3.5	235	9.5×10^4 (4.8)
βN158W[d]	−	59	1.3	540	1.5×10^4 (0.8)
βF148W[d]	++++	98	27	195	8.8×10^5 (45)
βY331W[e]	++++	95	20	70	1.8×10^6 (92)

[a] All mutations (except βY297W) were moved into plasmid p0W1 and expressed in strain AN888. Strain AN888 expresses no F_1 subunits. In plasmid p0W1 all natural tryptophans in F_1 have been replaced. Thus, in every case except βY297W, the introduced Trp is the only Trp in F_1. βY297W was expressed in plasmid pDP34N (see text) and in this case the natural Trp residues are still present. [b] Wild-type strain for the growth experiments was pDP34N/AN888; wild-type F_1 containing all the natural Trp was prepared from strain SWM1 (*26*). The Unc$^-$ strain was pUC118/AN888. [c] Value in parentheses is percent of wild-type k_{cat}/K_M. [d] Mutations were described previously (*22*). [e] As in ref *18*.

To increase the signal-to-noise ratio of the Trp fluorescence in purified mutant enzymes, we used Trp-free F_1 expressed from plasmid p0W1 (*24*) as background. Each new mutation was moved into plasmid p0W1 for expression, thus the newly introduced Trp residue was the sole Trp in each mutant enzyme (βY297W was an exception, see below).

Growth Properties of Strains Containing Novel Tryptophan Mutations. Effects of the novel Trp mutations on cell growth by oxidative phosphorylation were assayed by growth on plates containing succinate as sole carbon source and growth yields in liquid medium containing limiting (3 mM) glucose. Results are shown in Table 2. βY297W, βF410W, αF291W, and αF354W were all close to normal. βF404W was partially Unc$^+$ on succinate plates and in the growth yield test. Included in Table 2 for comparison are data for the mutations βF148W, βY331W, βV153W, and βN158W, generated previously.

Enzymatic Properties of Purified F_1. Purified F_1 of normal molecular size and subunit composition (as judged by the elution profile of the Sephacryl S-300 gel chromatography column used in the last purification step and by SDS−gel electrophoresis) was isolated from strains containing the new mutations βF404W, βF410W, αF291W, and αF354W, all expressed from plasmid p0W1 which lacks the natural F_1 Trp residues. In contrast, attempts to purify F_1 from the strain carrying the mutation βY297W in plasmid p0W1 resulted in very poor yield of enzyme. However, we were able to purify F_1 from the strain containing βY297W expressed from plasmid pDP34N, which contains the natural Trp residues, and fortunately the fluorescence signal of the β-Trp-297 residues in this enzyme was sufficiently large as to allow it to stand out over the wild-type signal.

Table 2 shows V_{max}, K_M, and k_{cat}/K_M values for ATPase activity of each of the new mutant enzymes. In all cases, the dependence of catalytic activity versus MgATP concentration could be fitted well to a model assuming a single K_M value. It is apparent that the enzymes showed largely normal characteristics. V_{max}(MgATP) was somewhat low in βY297W mutant F_1 (17% of wild-type), but differed from wild-type by a factor of ≤ 2 in the remaining cases (βF404W, 50%; βF410W, 71%, αF291W, 111%; αF354W, 129%). K_M-(MgATP) was close to wild-type in βY297W and αF291W mutant F_1 and increased by factors of 2−3 in the βF404W, βF410W, and αF354W enzymes. The resulting k_{cat}/K_M values varied between 17 and 165% of wild-type. For comparison, the previously determined values for the βV153W, βN158W, βF148W, and βY331W enzymes are also given in Table 2. The first two differ from wild-type significantly, and this was reflected in poor growth characteristics. The βF148W enzyme has somewhat elevated K_M (~2-fold), and the βY331W enzyme is essentially normal.

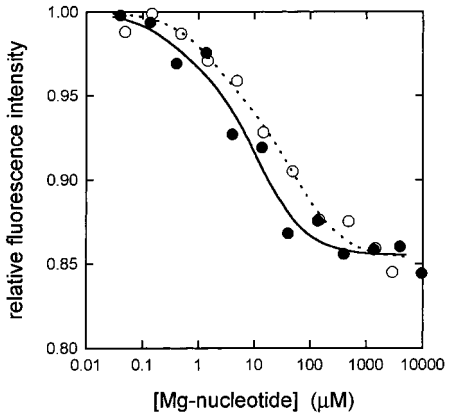

FIGURE 1: Nucleotide binding to βF404W mutant F_1. Change of the fluorescence signal (λ_{exc} = 295 nm, λ_{em} = 340 nm) upon addition of MgADP (○) or MgAMPPNP (●) is shown. The lines are fits of theoretical curves to the data points assuming a model with two types of binding site; dotted line, MgADP; solid line, MgAMPPNP. The calculated K_d values are given in Table 3. Further details are described in the text.

Fluorescence and Ligand-Binding Properties of Purified F_1 from Tryptophan Mutants. (*1*) *βF404W*. Purified F_1 containing β-Trp-404 as the sole Trp exhibited a corrected fluorescence spectrum with maximum at 333 nm (λ_{exc} = 295 nm), indicating a moderately hydrophobic environment of the Trp residues. Addition of MgADP, MgAMPPNP, or MgATP (all at 1 mM concentration) resulted in quenching of the fluorescence signal by 15%, accompanied by a blue-shift of 1 nm, indicating a small increase in hydrophobicity. The dependence of the fluorescence signal on concentration of MgADP or MgAMPPNP is shown in Figure 1. We compared models assuming either one or two types of binding site by fitting theoretical curves to the data points, and for both MgADP and MgAMPPNP, the results indicated that the model with two types of binding site was clearly superior. With MgADP, the fluorescence quenching associated with binding to the high-affinity type of site was 38% of the total signal change; with MgAMPPNP it was 23%. Thus, the data indicated the presence of one site of higher and two sites of lower affinity for both nucleotides. Such a binding pattern had been shown earlier for βY331W enzyme (*5*), where the fluorescence of the three β-Trp-331 residues is completely quenched upon binding of saturating MgADP or MgAMPPNP, and identical contribution of each of the three β-Trp-331 residues to the total signal was verified independently (*15*). Furthermore, the same binding model

Table 3: Nucleotide-Binding Properties of Novel Tryptophan Mutants

mutation	MgADP binding K_{d1} (μM)	MgADP binding $K_{d2,3}$ (μM)	MgAMPPNP binding K_{d1} (μM)	MgAMPPNP binding $K_{d2,3}$ (μM)	MgATP hydrolysis, K_M (μM)
βY297W	ND[a]	ND	0.06[d]	ND[d]	80
βF404W	1.9	58	0.35	12	265
βF410W	0.12	93	0.35	104	160
βV153W	0.03	53	0.06	225	235
βN158W	6.0	206	18	1300	540
αF291W	0.30	ND	0.34	ND	70
βF148W[b]	0.7	340	3.0	64	195
βY331W[c]	0.14	20	0.14	47	70

[a] ND, not determined due to lack of fluorescence response, see text. [b] From ref *22*. [c] From refs *5* and *18*. [d] Data given are for single-site model. See text for discussion.

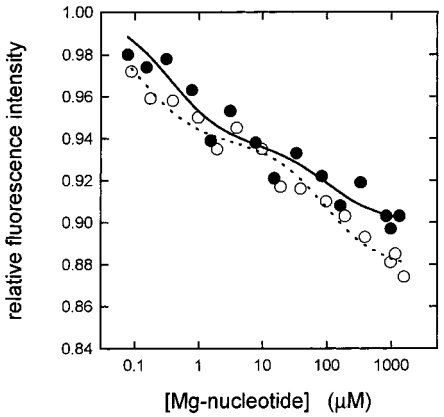

FIGURE 2: Nucleotide binding to βF410W mutant F_1. Change of the fluorescence signal (λ_{exc} = 295 nm, λ_{em} = 340 nm) upon addition of MgADP (○) or MgAMPPNP (●) is shown. The lines are fits of theoretical curves to the data points assuming a model with two types of binding site; dotted line, MgADP; solid line, MgAMPPNP. The calculated K_d values are given in Table 3. Further details are described in the text.

was shown by direct binding studies with radioactive MgAMPPNP, in which all three catalytic sites were filled, with one site of higher and two sites of lower affinity (*33*, *34*).

K_d values for binding of MgADP and MgAMPPNP to the βF404W enzyme are given in Table 3. Overall, it is apparent that in the βF404W mutant both nucleoside di- and triphosphate elicited the same type of fluorescence change, and although there are differences in the actual binding parameters, the βF404W mutant in general resembled βY331W.

(*2*) *βF410W*. The maximum of the corrected Trp fluorescence spectrum of βF410W mutant F_1 was also at 333 nm. Upon addition of 1 mM MgADP, MgAMPPNP, or MgATP, the emission spectrum was blue-shifted by about 1 nm, and the signal was quenched by 10−12%. As observed with βF404W above, titration with increasing concentration of MgADP or MgAMPPNP also indicated the presence of two types of site (Figure 2). However, in this case, the fluorescence quench associated with high-affinity binding was similar (50% of the total signal with MgADP, 60% with MgAMPPNP) to that for the lower affinity component. These results indicated that the β-Trp-410 residue at site one is quenched more strongly on addition of Mg-nucleotide that those at sites two and three. This enzyme

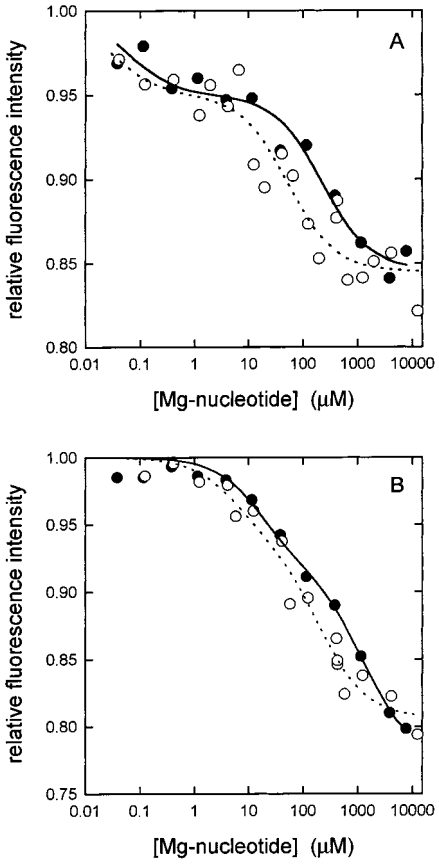

FIGURE 3: Nucleotide binding to βV153W and βN158W mutant F_1. (A) βV153W F_1; (B) βN158W F_1. Change of the fluorescence signal (λ_{exc} = 295 nm, λ_{em} = 340 nm) upon addition of MgADP (○) or MgAMPPNP (●) is shown. The lines are fits of theoretical curves to the data points assuming a model with two types of binding site; dotted line, MgADP; solid line, MgAMPPNP. The calculated K_d values are given in Table 3. Further details are described in the text.

showed normal V_{max} and K_M(MgATP) values (Table 2), and as noted above, the fluorescence change on addition of saturating (1 mM) MgATP, MgADP, or MgAMPPNP was the same. It is firmly established that saturating concentrations of nucleotide fill all three catalytic sites in normal enzyme (*4*, *5*); therefore, there is no doubt that all three nucleotides bind to all three catalytic sites in the βF410W enzyme also.

The calculated K_d values for binding of MgADP and MgAMPPNP to βF410W F_1 are given in Table 3. While the actual binding parameters are not the same, in general βF410W enzyme was similar to βF404W and βY331W in behavior.

(*3*) *βV153W and βN158W*. The Trp fluorescence properties of βV153W and βN158W mutant F_1 were described previously (*22*). Both Trp residues are located in a highly hydrophobic environment (emission maximum of βV153W, 325 nm; βN158W, 322 nm). Upon addition of 1 mM MgADP, MgATP, or MgAMPPNP, the Trp fluorescence of the βV153W mutant enzyme was quenched by about 15% and that of the βN158W mutant by approximately 20%.

Here, we investigated in detail the dependence of the fluorescence responses on the concentration of MgADP and MgAMPPNP (Figure 3). For both mutant enzymes and both nucleotides, the titration curves indicated the presence of two classes of binding sites, with one site of higher and two sites

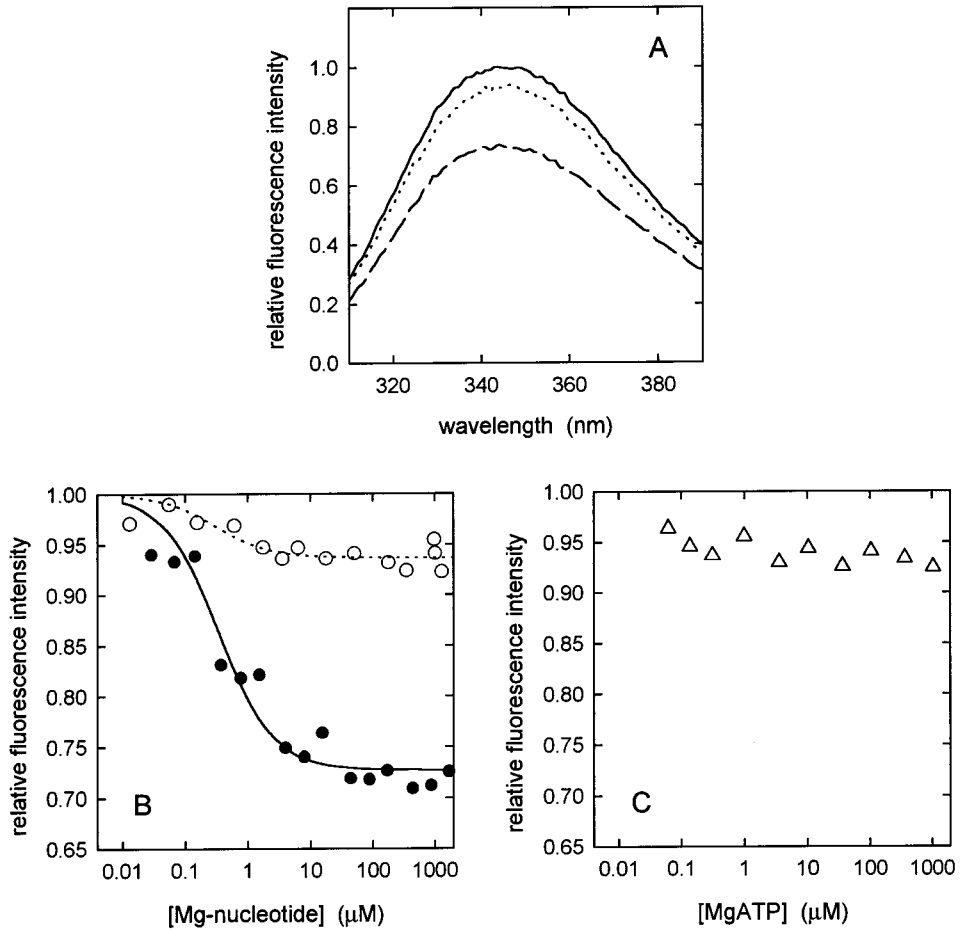

FIGURE 4: Fluorescence spectra and nucleotide binding characteristics of αF291W mutant F_1. (A) Trp fluorescence spectra (uncorrected; $\lambda_{exc} = 295$ nm) of αF291W mutant F_1 in absence of added nucleotide (solid line), in the presence of 1 mM MgAMPPNP (dashed line), and in the presence of 1 mM MgADP (dotted line). (*B*) Change of the fluorescence signal ($\lambda_{em} = 340$ nm) upon titration with MgADP (○) or MgAMPPNP (●); the lines are fits of theoretical curves to the data points assuming a model with a single type of binding site; dotted line, MgADP; solid line, MgAMPPNP. The calculated K_d values are given in Table 3. Further details are described in the text. (C) Change of the fluorescence signal ($\lambda_{em} = 340$ nm) of the enzyme upon titration with MgATP.

of lower affinity, and the higher affinity site contributing 32−37% of the total fluorescence quench. Calculated K_d values are given in Table 3. In the βN158W enzyme, perturbation of the nucleotide-binding parameters was significant, but this is not unexpected given that enzyme activity was low (Table 2). It is to be noted, however, that in both cases the nucleotide-binding pattern was similar to that seen in βY331W, βF404W, and βF410W, i.e., the same fluorescence response was observed on addition of nucleoside di- or triphosphate, with one site of higher and two sites of lower affinity.

(*4*) α*F354W*. The αF354W mutant F_1 showed an emission maximum at 331 nm ($\lambda_{exc} = 295$ nm). Addition of 1 mM MgADP, MgAMPPNP, or MgATP elicited neither a shift of the fluorescence spectrum nor any significant change in fluorescence intensity. Thus, this introduced Trp residue was insensitive to nucleotide occupancy of catalytic sites.

(*5*) α*F291W*. The corrected Trp fluorescence spectrum of αF291W mutant F_1 exhibited a maximum at 332 nm, indicating an environment of moderate hydrophobicity. Upon addition of 1 mM MgADP, the fluorescence signal was quenched maximally by ∼7%, without noticeable shift of the emission maximum (Figure 4A). Titration with MgADP revealed that the fluorescence response reached saturation at MgADP concentration of a few micromolar (Figure 4B). A good fit of a theoretical curve to the measured data points was obtained using a binding model with a single type of site ($\Delta F = -6.3\%$; $K_d = 0.30$ μM; dotted line in Figure 4B). From comparison of this K_d value with other values in Table 3, it was obvious that the fluorescence quenching seen corresponded to binding of MgADP at the first, high-affinity catalytic site and that binding to the two sites of lower affinity produced no significant further fluorescence change.

MgAMPPNP caused much stronger quenching of fluorescence than MgADP. Addition of 1 mM MgAMPPNP decreased the fluorescence signal by nearly 30%, without a significant shift in the emission maximum of the spectrum (Figure 4A). Titration with MgAMPPNP showed that, already at MgAMPPNP concentration of a few micromolar, the signal had reached saturation (Figure 4B). A satisfactory fit was obtained using a model with a single type of binding site ($\Delta F = -27\%$; $K_d = 0.34$ μM; Figure 4B, solid line). Thus, the fluorescence response of αF291W mutant F_1 with MgAMPPNP was also due predominantly, if not exclusively, to conformational changes occurring at catalytic site 1.

Titration of αF291W mutant F_1 with MgATP is shown in Figure 4C. At saturating MgATP concentration, the fluorescence signal decrease was about 7%, the same as that obtained with MgADP. Moreover, at concentrations of

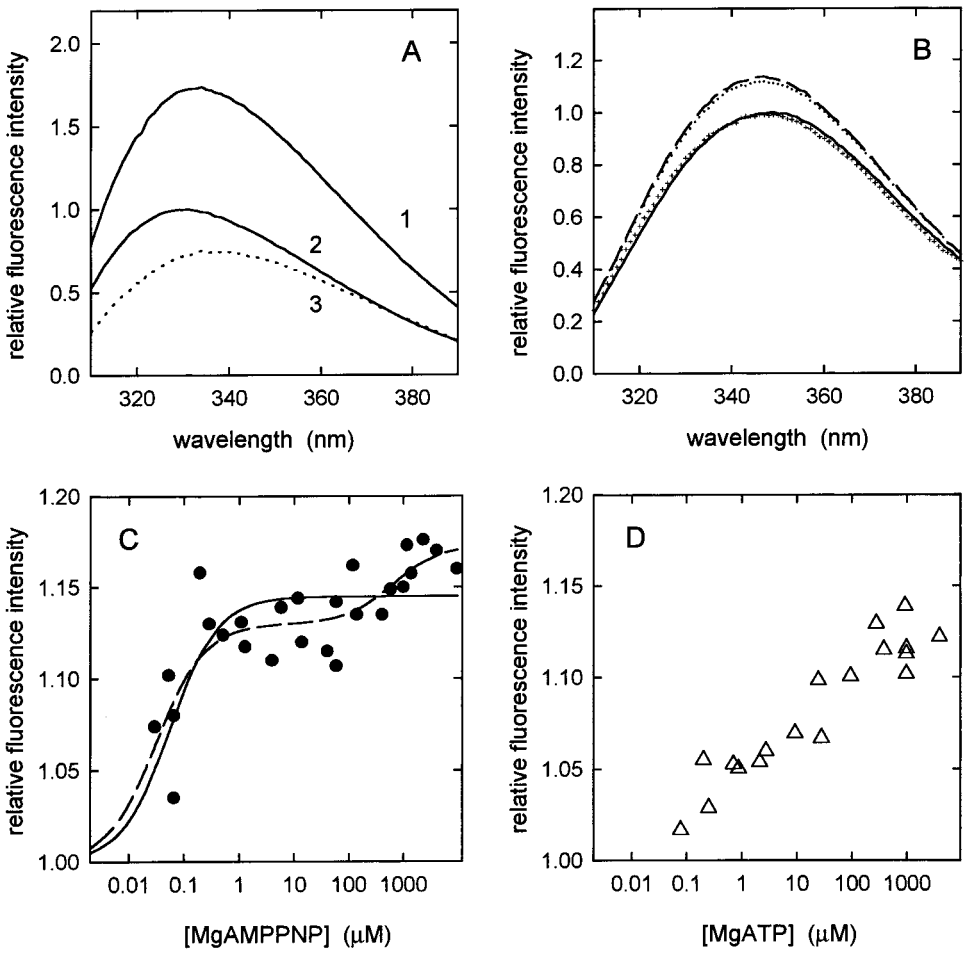

FIGURE 5: Fluorescence spectra and nucleotide binding characteristics of βY297W mutant F_1. (A) Trp fluorescence spectra (corrected; λ_{exc} = 295 nm) of βY297W (curve 1) and wild-type F_1 (curve 2); the spectra were adjusted to represent the same protein concentration. Curve (3) is the difference spectrum [mutant (curve 1) minus wild-type (curve 2)], representing the spectrum of the introduced β-Trp-297 residues. (B) Trp fluorescence spectra (uncorrected) in absence of added nucleotides (—), in the presence of 1 mM MgADP (+), 1 mM MgAMPPNP (- - -), and 1 mM MgATP (•••). (C) Change of the fluorescence signal (λ_{em} = 340 nm) of the enzyme upon titration with MgAMPPNP; the solid line is a fit of a theoretical curve to the data points assuming a model with one type of binding site; the dotted line is a fit of a theoretical curve to the data points assuming a model with two types of binding site. The calculated K_d value is given in Table 3. Further details are described in the text. (D) Change of the fluorescence signal of the enzyme (λ_{em} = 340 nm) upon titration with MgATP.

around 0.1 μM MgATP, the response was already close-to-maximal; the K_d(MgATP) was estimated to be <20 nM, indicating that, as with MgADP and MgAMPPNP, the fluorescence response was due virtually completely to binding at the first, high-affinity catalytic site. Since the K_M(MgATP) of the αF291W enzyme is 70 μM, which is similar to βY331W (and wild-type), and it is fully established that K_M(MgATP) corresponds to binding at the third catalytic site (*4*, *5*), there is no doubt that all three catalytic sites do fill with MgATP in this enzyme. At 1 mM MgATP concentration, the highest used in the titration (Figure 4C), the enzyme would be undergoing steady-state catalysis at V_{max}. It is apparent that under these conditions the environment that residue α-Trp-291 in the high-affinity catalytic site is experiencing, in time-average, appears to be very similar to that when the high-affinity site is filled with MgADP and not that with MgAMPPNP.

(*6*) *βY297W*. As described above, it was necessary to use wild-type containing the nine natural Trps as background for this mutation, because the yield of F_1 obtained in the Trp-free background was very poor. Figure 5A shows the corrected Trp fluorescence spectrum of βY297W mutant F_1. The difference spectrum (βY297W mutant minus wild-type enzyme; curve 3 in Figure 5A) exhibited a maximum at 338 nm, indicating a moderately polar environment for the introduced β-Trp-297 residues.

Addition of 1 mM MgADP resulted in a slight blue-shift (1−2 nm) of the spectrum, suggesting a slight decrease in the polarity, without significant change in signal intensity (Figure 5B). Addition of 1 mM MgAMPPNP also gave a small blue-shift (2 nm), together with an increase of the overall fluorescence intensity of about 15% (at λ_{em} = 340 nm), which corresponds to an increase of the β-Trp-297 fluorescence of 35%. Addition of 1 mM MgATP (Figure 5B) also gave an increase of fluorescence, similar to that seen with MgAMPPNP.

Investigation of dependence of the fluorescence increase on MgAMPPNP concentration showed that the major portion of the response occurred at concentrations of ≤1 μM (Figure 5C). The solid line represents the fit obtained assuming a model with a single type of binding site, yielding a K_d of 0.06 μM and a fluorescence increase at saturation (ΔF) of +14.5%. The dashed line represents the fit obtained assuming a model with two types of binding sites, yielding K_{d1} = 0.03 μM (ΔF = +13%) and K_{d2} = 630 μM (ΔF = +4%). Due to the scatter in the data, both models appear

equally valid. However, comparison with the results obtained in the other Trp mutants (Table 3) indicates that the K_d of 0.06 or 0.03 μM reflects binding to the first, high-affinity catalytic site. This means that the β-Trp-297 residue at catalytic site 1 shows a strong fluorescence response to MgAMPPNP binding ($\Delta F = 14.5$ or 13%, depending on the model chosen), whereas those at sites 2 and 3 show at most a small fluorescence response.

The dependence of the β-Trp-297 fluorescence signal on increasing MgATP concentration is shown in Figure 5D. The increase in fluorescence was gradual, reaching a maximum of +12% at 1−4 mM MgATP. This concentration corresponds to steady-state, V_{max} hydrolysis conditions since K_M(MgATP) for βY297W mutant F_1 was 80 μM. Given that the K_M(MgATP) is the same as that for wild-type and βY331W, the three catalytic sites would be filled under these conditions. Therefore, in this mutant, the substituted Trp experiences an environment in the first, high-affinity catalytic site under steady-state turnover conditions similar to that induced by MgAMPPNP.

DISCUSSION

General. We introduced novel Trp residues surrounding the bound nucleotide in the catalytic site of *E. coli* F_1-ATPase, using the X-ray structure of the MgAMPPNP-containing site as a guide, to obtain new information concerning the catalytic site environment and enzyme mechanism. Trp residues were positioned close to the adenine ring, ribose, α/β-phosphates, and γ-phosphate. Purified mutant F_1-ATPase enzymes were obtained and their fluorescence properties characterized. In the majority of cases (Table 2), the enzymes showed relatively normal catalytic characteristics and can be expected to function according to the same mechanism as wild-type. One possible exception to this statement was the βN158W mutant (Table 2), but in this case, the fluorescence behavior was not particularly remarkable.

Most of the substituted Trp residues reported a moderately nonpolar environment in the empty catalytic site (λ_{max} of fluorescence 331−333 nm), which became slightly more nonpolar on binding of nucleotide. Residues β-Trp-153 and β-Trp-158, which are buried to greater extent than any of the other Trp substitutions, registered the most hydrophobic environments. Residue β-Trp-297 reported the most polar environment (λ_{max} 338 nm), consistent with its location close to the γ-phosphate. In the X-ray structure, residue β-Tyr-297 appears to form an insulating "wall" at the side of the pocket where the γ-phosphate, Mg^{2+}, and putative attacking water molecule are located. Interestingly, none of the new Trp substitutions described here was in an environment anywhere near as polar as that of β-Trp-331 [fluorescence maximum at 349 nm (*5*)], which stacks directly against the adenine ring of bound nucleotide in occupied catalytic sites, but appears to be fully exposed to an aqueous environment in unoccupied sites.

Three Classes of Tryptophan Substitutions. On the basis of the observations made, we can separate the new Trp substitutions loosely into three groups. In the first group are βF404W, βF410W, βN158W, and βV153W. The first three are positioned within 4−7.5 Å of the adenine ring, while βV153W is 5 Å from the α/β-phosphates. These mutations all share the following properties, which are seen also in βY331W. Each one gives the same fluorescence response with MgADP, MgAMPPNP, or MgATP. Titration with MgADP reveals a pattern of binding consisting of one site of higher and two sites of lower affinity, with the K_d at the higher affinity site being in the submicromolar or low micromolar range, and the K_d at the lower affinity sites being in the range of K_M(MgATP). Titration with MgAMPPNP reveals a pattern of binding similar to that seen with MgADP. In the βF404W, βN158W, and βV153W enzymes, the quenching of fluorescence was the same or similar at each of the three catalytic sites, as was found earlier with the βY331W enzyme, but the βF410W enzyme showed a stronger fluorescence quench when nucleotide bound at site one than at sites two and three. One conclusion emphasized by this group of mutants is that in the absence of catalytic turnover (with MgADP or MgAMPPNP), where there would be no rotation of the γ-subunit, sites two and three appear similar. The five residues β-404, β-410, β-153, β-158, and β-331 are shown in Figure 6 in yellow. It is readily apparent that they cluster around the nucleotide in a region away from the seat of catalysis.

In the second group is α-Trp-354. This residue lies on α-subunit at the α/β-interface, 12 Å from the ribose, and is shown in grey in Figure 6. Unfortunately, it gave no change in fluorescence signal with any nucleotide.

In the third group are αF291W and βY297W, which lie 10 and 6 Å, respectively, from the γ-phosphate. Both gave a completely different fluorescence response to MgADP versus MgAMPPNP, and in this respect, they resemble the βF148W mutation described previously (*22*). In Figure 6, we have shown each of the residues β-148, β-297, and α-291 in red, and it is readily apparent that these three residues cluster in the region close to the γ-phosphate. This region therefore undergoes differential conformational changes depending on the species of nucleotide bound, whereas the regions occupied by the residues in yellow do not. This is consistent with previous evidence (reviewed in ref *2*) that it is primarily the liganding around the Mg^{2+} and the γ-phosphate that generates catalytic site binding asymmetry and facilitates catalysis. Figure 6 also provides information to guide where other types of reporter probe might be inserted in the molecule, depending on the type of information that is being sought.

Direct Detection of the High-Affinity Catalytic Site during Multisite, Steady-State Catalysis. A second, distinctive feature of the αF291W and βY297W mutations was that the fluorescence response measured on binding of MgADP or MgAMPPNP was almost exclusively (αF291W) or predominantly (βY297W) due to the Trp residue in the first, high-affinity catalytic site. As we noted in the introductory portion of this paper, current models of the catalytic mechanism of F_1-ATPase postulate that during steady-state catalysis at V_{max} only one site is catalytically active at any one time and that this site corresponds to the high-affinity site identified in "unisite" experiments (*2*, *8*−*10*). It has not been possible up to now to detect whether this site actually exists during steady-state catalysis at the concentration of MgATP necessary to fill all three catalytic sites and achieve V_{max} turnover rate. MgATP titrations were performed here with αF291W and βY297W mutations, and, in both cases, fluorescence signals corresponding to the high-affinity catalytic site were

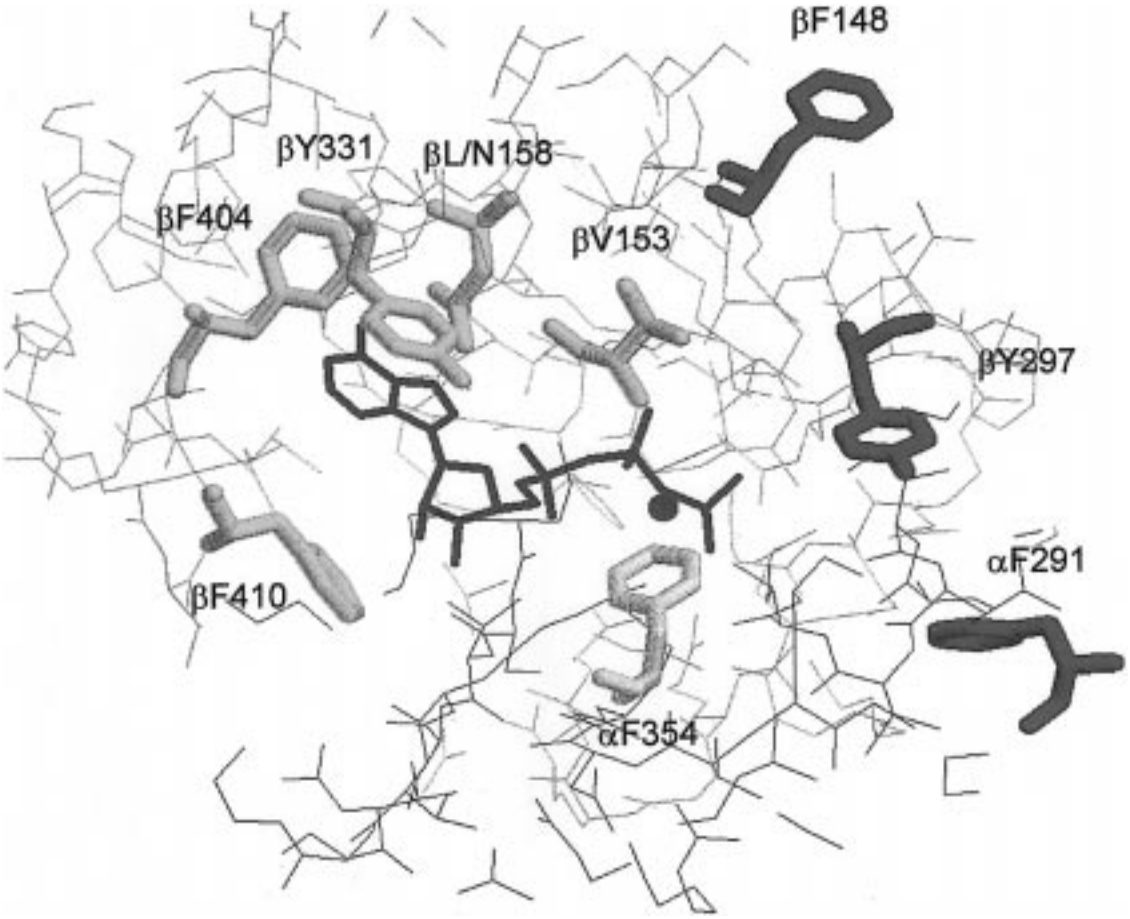

FIGURE 6: Trp residues at the catalytic site of F_1-ATPase and their differential responses to nucleotide binding. The environment of the MgAMPPNP-occupied catalytic site (*3*) is shown, displayed using RasMol software kindly provided by Dr. Roger Sayle (Glaxo Research and Development, Greenford, U.K.). Mg^{2+} and AMPPNP are depicted in green. Residues which have been replaced by Trp (*5*, *22*; this study) are shown as stick models; residue β-158 is Asn in *E. coli* F_1, but is shown here as Leu as in the mitochondrial enzyme. Replacement of a residue shown in yellow resulted in a Trp which gave the same response to binding of MgADP, MgAMPPNP, or MgATP. Replacement of a residue depicted in red produced a Trp with responded differently to binding of MgADP versus MgAMPPNP. Substitution of residue α-Phe-354 (grey) resulted in a Trp which did not change its fluorescence upon binding of nucleotides to the catalytic site. Background residues shown as grey wireframe belong to the β-subunit, those in purple belong to the adjacent α-subunit.

seen at MgATP concentration sufficient to achieve V_{max}. Therefore, an important conclusion from this work is that the high-affinity site is present in the steady state.

Interpretation of the actual fluorescence changes in the αF291W and βY297W mutants is not, however, straightforward. In αF291W, the substituted Trp showed a large quench of fluorescence (~30%) with MgAMPPNP and a smaller quench (7%) with MgADP. With MgATP, the maximum response was achieved at very low concentration and corresponded in amplitude to that of MgADP, as if the Trp in the high-affinity catalytic site were "seeing" predominantly MgADP. In βY297W, the substituted Trp showed no change in fluorescence intensity with MgADP, and around 15% enhancement of fluorescence with MgAMPPNP. With MgATP, the maximum fluorescence response resembled that of MgAMPPNP, but was not achieved until saturating MgATP was present. Several different conformers of the high-affinity catalytic site must exist (containing, e.g., MgADP + Pi, an MgADP·Pi transition state, MgATP), and it is difficult to predict at this time the response of a fluorescent probe to one or more of them. The X-ray structure (*3*) demonstrates that both α-Phe-291 and β-Tyr-297 undergo large spatial displacements when the empty catalytic site (β_E) binds nucleotide, but hold similar positions in both β_{DP} and β_{TP} catalytic sites. Future work on these mutants may be expected to clarify this issue, and to yield information about the behavior of the high-affinity site under steady-state conditions.

Summary. Trp substitutions surrounding the nucleotide bound in catalytic sites of F_1 report the environment in different subdomains of the site and show different patterns of fluorescence response depending on relative location. Two novel Trp substitutions proximate to the γ-phosphate showed differential fluorescence responses toward MgADP and MgAMPPNP and responded specifically to the first, high-affinity catalytic site. Titrations with MgATP confirmed the presence of the high-affinity site under steady-state hydrolysis conditions.

REFERENCES

1. Nakamoto, R. K. (1996) *J. Membr. Biol. 151*, 101−111.
2. Weber, J., and Senior, A. E. (1997) *Biochim. Biophys. Acta 1319*, 19−58.
3. Abrahams, J. P., Leslie, A. G. W., Lutter, R., and Walker, J. E. (1994) *Nature 370*, 621−628.
4. Löbau, S., Weber, J., and Senior, A. E. (1998) *Biochemistry 37*, 10846−10853.
5. Weber, J., Wilke-Mounts, S., Lee, R. S. F., Grell, E., and Senior, A. E. (1993) *J. Biol. Chem. 268*, 20126−20133.

6. Noji, H., Yasuda, R., Yoshida, M., and Kinosita, K., Jr. (1997) *Nature 386*, 299−302.
7. Yasuda, R., Noji, H., Kinosita, K., Jr., Motojima, F., and Yoshida, M. (1997) *J. Bioenerg. Biomembr. 29*, 207−209.
8. Boyer, P. D. (1993) *Biochim. Biophys. Acta 1140*, 215−250.
9. Cross, R. L., and Duncan, T. M. (1996) *J. Bioenerg. Biomembr. 28*, 403−408.
10. Penefsky, H. S., and Cross, R. L. (1991) *Adv. Enzymol. 64*, 173−214.
11. Van Raaij, M. J., Abrahams, J. P., Leslie, A. G. W., and Walker, J. E. (1996) *Proc. Natl. Acad. Sci. U.S.A. 93*, 6913-6917.
12. Abrahams, J. P., Buchanan, S. K., Van Raaij, M. J., Fearnley, I. M., Leslie, A. G. W., and Walker, J. E. (1996) *Proc. Natl. Acad. Sci. U.S.A. 93*, 9420−9424.
13. Shirakihara, Y., Leslie, A. G. W., Abrahams, J. P., Walker, J. E., Ueda, T., Sekimoto, Y., Kambara, M., Saika, K., Kagawa, Y., and Yoshida, M. (1997) *Structure 5*, 825−836.
14. Löbau, S., Weber, J., Wilke-Mounts, S., and Senior, A. E. (1997) *J. Biol. Chem. 272*, 3648−3656.
15. Weber, J., Wilke-Mounts, S., and Senior, A. E. (1994) *J. Biol. Chem. 269*, 20462−20467.
16. Weber, J., and Senior, A. E. (1996) *J. Biol. Chem. 271*, 3474-3477.
17. Weber, J., Wilke-Mounts, S., Grell, E., and Senior, A. E. (1994) *J. Biol. Chem. 269*, 11261−11268.
18. Weber, J., and Senior, A. E. (1995) *J. Biol. Chem. 270*, 12653−12658.
19. Weber, J., Bowman, C., Wilke-Mounts, S., and Senior, A. E. (1995) *J. Biol. Chem. 270*, 21045−21049.
20. Weber, J., and Senior, A. E. (1997) *FEBS Lett. 412*, 169−172.
21. Weber, J., Hammond, S. T., Wilke-Mounts, S., and Senior, A. E. (1998) *Biochemistry 37*, 608−614.
22. Weber, J., Bowman, C., and Senior, A. E. (1996) *J. Biol. Chem. 271*, 18711−18718.
23. Vandeyar, M., Weiner, M., Hutton, C., and Batt, C. (1988) *Gene 65*, 129−133.
24. Wilke-Mounts, S., Weber, J., Grell, E., and Senior, A. E. (1994) *Arch. Biochem. Biophys. 309*, 363−368.
25. Weber, J., Lee, R. S. F., Grell, E., Wise, J. G., and Senior, A. E. (1992) *J. Biol. Chem. 267*, 1712−1718.
26. Rao, R., Al-Shawi, M. K., and Senior, A. E. (1988) *J. Biol. Chem. 263*, 5569−5573.
27. Laemmli, U. K. (1970) *Nature 227*, 680−685.
28. Bradford, M. M. (1976) *Anal. Biochem. 72*, 248−254.
29. Senior, A. E., Latchney, L. R., Ferguson, A. M., and Wise, J. G. (1984) *Arch. Biochem. Biophys. 228*, 49−53.
30. Taussky, H. H., and Shorr, E. (1953) *J. Biol. Chem. 202*, 675−685.
31. van Veldhoven, P. P., and Mannaerts, G. P. (1987) *Anal. Biochem. 161*, 45−48.
32. Pecoraro, V. L., Hermes, J. D., and Cleland, W. W. (1984) *Biochemistry 23*, 5262−5271.
33. Wise, J. G., Duncan, T. M., Latchney, L. R., Cox, D. N., and Senior, A. E. (1983) *Biochem. J. 215*, 343−350.
34. Cross, R. L., and Nalin, C. M. (1982) *J. Biol. Chem. 257*, 2874−2881.

BI981089C